Scientific Research and Essays Vol. 6(31), pp. 6554-6565, 16 December, 2011
Available online at http://www.academicjournals.org/SRE
DOI: 10.5897/SRE11.1650
ISSN 1992-2248 ©2011 Academic Journals

Full Length Research Paper

Automatic Spike detection and correction for outdoor machine vision: Application to tomato

Nasrolah Sahragard[1], Abdul Rahman Bin Ramli[2], Mohammad Hamiruce Bin Marhaban[3] and Shattri Bin Mansor[4]

[1]Intelligent System and Robotics Laboratory, Institute of Advanced Technology, University Putra Malaysia 43400 Serdang, Selangor, Malaysia And Depatrment of Electrical and Computer Engineering, Hormozgan University, Bandar Abbas, Iran.
[2]Department of Computer and Communication Systems, Faculty of Engineering, University Putra Malaysia 43400 Serdang, Selangor, Malaysia.
[3]Department of Electrical and Electronic Engineering, Faculty of Engineering, University Putra Malaysia 43400 Serdang, Selangor, Malaysia.
[4]Department of Civil Engineering, Faculty of Engineering, University Putra Malaysia 43400 Serdang, Selangor, Malaysia.

Accepted 31 October, 2011

The use of outdoor machine vision has become part of the technology used in industry, farming, and military. Applications include color recognition such as obstacle detection, road following, and landmark recognition. This study proposes a spike auto-detection and correction technique based on color modeling and surface reflectance to predict the color and correct the spike region apparent color on the tomato surface. This algorithm classifies tomatoes in red, orange, and green color category based on training images with accuracy of 94%. Then by the use of mean shift color segmentation algorithm, the spiky pixels on the surface of tomato are spotted. Based on the color model and Normalized Photometric Function (NPF) for relevant tomato in a tropical place as Malaysia, the color of each spiky pixel is estimated in HSV (hue, saturation, and value) color space. Finally, the specular effects are corrected through replacing their estimated color. From the experimental results, this study demonstrates overall accuracy of 93%. The contribution of the paper lies in the use of outdoor color based models for tropical places as previously developed by the authors to correct the specular effects on a spherical surface such as tomato.

Key words: Color imaging, colorimetry, color models, glossy reflection, surface reflection functions.

INTRODUCTION

When sun is visible and the geometry of an object's surface is in such a way that the angle between the viewing and incident is zero, there is a spike spot created on the surface of certain objects which are capable of showing specular effects. Theoretically, when light rays strike a surface, some of the rays will reflect back into the air, and the rest of light rays will penetrate the body of surface. Some of the light go through the body and the others will reflect back onto the surface and then into the air. The light rays that are immediately reflected are called specular or interface reflections. The ones that have penetrated and reflected back into the air are called diffuse or body reflections. There is yet another kind of reflection called specular spike. Usually this kind of reflection is ignored in inhomogeneous objects since its presence is very minor. There are smooth surfaces such as road signs that are able to have specular spike effect. In recognition and road following tasks it is crucial to deal with the spike in the image. This effect can be observed when the angle between the incident light and viewing ray is zero.

This paper explains how to detect and remove the

*Corresponding author. E-mail: Sahragard@yahoo.com.

spike effect in the image acquired by an outdoor vision system. This correction method will help algorithms used for outdoor machine vision to function correctly when the situation arises. Based on a series of experiments, a daylight color model is built for a tropical place as Malaysia showing the color of daylight illumination during the day. Also, for each class of tomatoes (Red, Orange, and Green) a Normalized Photometric Function (NPF) is built which relates the relative viewing angle and the normalized HSV distance between the lambertian color and the illuminant color. For the application of tomato, a classifier is built to distinguish between the red, orange, and green tomatoes. The spike region is located by applying the Comaniciu and Meer (2002) segmentation Mean Shift algorithm. Finally, by the use of color model and NPF model, the color of the spiky pixels are estimated and recovered. The building of context color based models for outdoor scenes in Malaysia to estimate surface color and actually apply them to outdoor images of spherical objects is the main contribution of this paper.

There are a number of different algorithms to correct images taken by regular cameras. Some of these algorithms refer to illumination correction to affect the quality of images for computer vision. For example Wu et al (2010) proposed an image illumination correction algorithm combining tone mapping and space decomposition based on adjusting brightness. There is no need for image transformation and image statistic information. So the computational complexity is reduced and it is easy to implement in hardware. Applying this algorithm will remove the impact of illumination, and enhance the quality of the image. Also Tu et al. (2010) proposed a new variation of Retinex algorithm which is based on adaptive smoothing filter to get rid of varying illumination in color images. It is necessary to filter the changing illuminant in color images. The input image is convolved with adaptive smoothing mask windows to estimate illumination. The weight of each mask is calculated by combining measures of the illumination discontinuity at each pixel. By doing this, an illuminant estimation image is obtained from the original illuminant contaminated image. Then, illumination estimation image is removed from original image by using Retinex theory and get the final image. Good results are obtained.

Tan and Ikeuchi (2005a) came up with a method for highlights removal that used no segmentation or polarization filter. Highlights usually seen in inhomogeneous objects are combinations of diffuse and specular components. Their method produces an image with no specular components but keeps its geometrical information and there is a change in color value. The highlight free pixels are determined by using the logarithmic differentiation between the specular free image and the input image. Next, the specular component for each pixel is removed locally using a maximum of two pixels. A requirement for their method is to locate local color discontinuities. And since it fails to detect a considerable number of discontinuities then the final result could not be correct. In dealing with this problem, Tan and Ikeuchi (2005b) proposed a method using global approaches in place of local ones. This method effectively uses the input image coefficients of reflectance basis functions and its image with no specular component. The coefficients are combined to find the diffuse coefficients for pixels with the specular component. Another decomposing reflections algorithm is the work of Lin et al. (2002). Their work is based on color analysis and multi-baseline stereo. Here the specular pixels are identified by a voting-based multiple tri-view color histogram differencing.

In a different algorithm Chang and Tseng (2011) developed a technique to auto-detect and inpaint to correct overexposed faces in digital photography. Overexposed images are resulted by using flash when there is low atmospheric lighting. They get highlight information through applying different algorithms to detect bright spots and then inpainting techniques are done to do corrections. The input image undergoes a few steps such as face recognition detection, glossy reflection and oily face detection, glossy reflection detection compensation, and skin correction and inpainting to produce the output image. The output image is visually appealing and the glossy reflections are diminished. The inpainting process that Chang and Tseng (2011) have used is based on color mathematical morphology, as a traditional inpainting which propagates boundary values. From the sample images they used, it is obvious that the images are taken under controlled illumination. But in the case of outdoor environment, the specular surfaces may have different colors (for uniformly colored surface it has different shading of one color), so Chang and Tseng's method cannot be used since it replaces the glossy pixels by the neighboring pixel color where the neighboring pixels definitely have different color under varying illumination. Although all of the above methods and many other related algorithms deal with color correction of images, but none really address the issue of spike removal and color correction for outdoor machine images.

PROPOSED METHOD

Here the automatic spike detection and correction for outdoor machine vision is explained. In order to detect the spike pixels and perform correction in images being taken by outdoor machines, this study uses the Dorin and Meer (2002) segmentation algorithm to locate the spike region, followed by color predicting technique for corrections. Alternatively, a segmentation method is proposed by Sojodishijani et al. (2010). To estimate the apparent surface color of objects in images taken under outdoor environment, a color model specifically built for tropical region as Malaysia is used along with the Normalized Photometric Function (NPF) is also already built under the same conditions. By using the color model and the NPF for the proper tomato, the color of specular spike pixels are estimated and then used to correct the color of those faulty pixels.

Figure 1 shows the block diagram of the proposed method. The

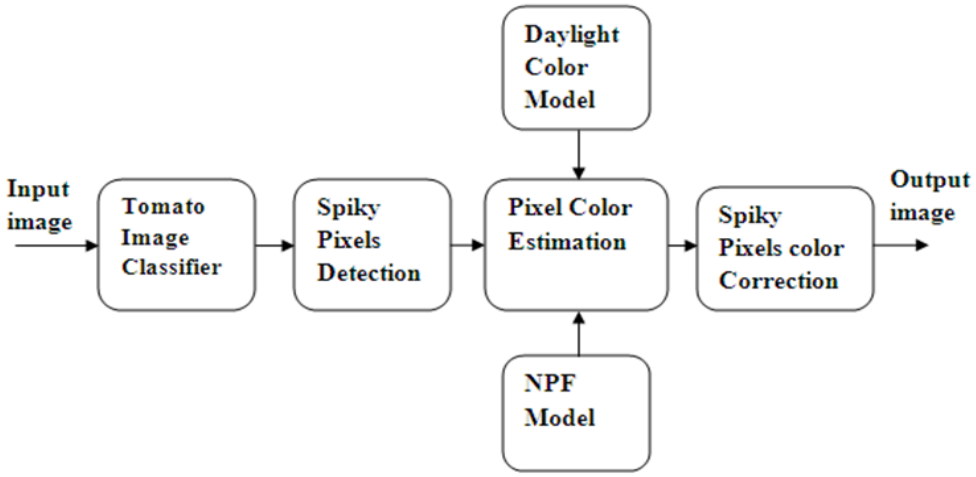

Figure 1. The block diagram of auto detection and correction of specular effects.

experiment involves a number of major steps as follows:

1. Input image
2. Tomato image classifier
3. Spiky pixels detection
4. Outdoor daylight color model, NPF model, and Tomato color estimation
5. Spiky pixels color correction
6. Output image

Input image: Color images containing spike effect on the surface of tomato are fed into the system as input image.

Tomato image classifier: Histogram based classifier is built to distinguish between the colors of the tomatoes as it will be needed in the treatment of color later during the color correction process. The classifier is built based on the color of 15 training images (64 x 64 pixels) from the tomato database images for each class of tomato color and it has the classification accuracy of 94%. The steps in building this classifier involve: i) building a function which is histogram generator in HSV color space for the 15 training images and normalize the histograms, ii) building a function that makes a vector of histograms of images based on grid size of 16 pixels and overlap of 4 pixels, and iii) build a matching histogram to compare the vector of histograms generated in steps i and ii. Then find the difference of the vectors and compare to a threshold value. There is some tuning involved in determining the best threshold value to make the classifier work efficiently.

Spiky pixels detection: By applying the mean shift segmentation algorithm proposed by Comaniciu and Meer (2002) the spike region locations are determined. The boundary of tomato is found using the canny edge detection and color threshold. If the spiky pixels locations are within the boundary of tomato then those are the candidate pixels on the surface of tomato to be color corrected. The code for the image segmentation algorithm which is developed with graphical interface is used and is available at http://server.cs.ucf.edu/~vision/source.html.

Outdoor daylight color model, NPF model, and Tomato color estimation: The prediction of tomato color is done by the use of three previously developed steps which are explained briefly in the following. These steps are the outdoor color model specifically built for a tropical place as Malaysia, the Lambert tomato surface color estimation bases on color coefficient matrix, and the Normalized Photometric Functions for the three different tomatoes. Then by using the outdoor color model to get the color of the illumination and the normalized HSV distance from the NPF model, the color of specified pixels are estimated based on the following relation:

$$A(n) = L + (I - L) * \rho \quad (1)$$

Where A is the estimated apparent color of a pixel at relative viewing angle n, L is the estimated Lambertian color, I is the illuminant color, and ρ is the relative normalized HSV distance. The relative viewing angle is provided by the user or an external system. Knowing the daylight condition, the daylight table could be used to get the illuminant color. Lambertian color L of a surface is estimated through experiments presented below. And finally the relative normalized HSV distance ρ comes from the Normalized Photometric Function for a surface. The normalized HSV distance (ρ) really determines how far a pixel color is estimated from Lambertian color and toward the illuminant on the Dichromatic line IL (line connecting I and L).

Spiky pixels color correction: Once the spiky pixel is located and its color is estimated then its color can be recovered by the estimated color for that pixel. This is done for all the pixels which showed specular spike effect and are located on tomato surface in step 3.

Output image: After color correction a new image is produced where the spiky spots on the surface of tomato are color corrected.

Building context outdoor color model in HSV color space

This outdoor color model is specially built for tropical region of Malaysia Sahragard et al. (2011). A table of daylight color in the direction of the sun and away from the sun and is indexed by sun angle, percentage of cloud cover, and sun visibility is constructed. The change in sun angle is from 0° to 90° partitioned into six groups (0°-10°, 11°-25°, 26°-45°, 46°-60°, 61°-75°, 76°-90°). Amount of cloud cover is also considered in four groups (0-20%, 21-50%, 51-70%, 71-100%). The sun visibility is recorded as 1 for visible sun, 0.5 for the sun covered with thin cloud and 0 for the total sun covered with clouds.

Figure 2. Apparatus used in building daylight color model with the white Munsell N/9 paper.

Table 1. Partial representation of daylight color model for tropical regions showing normalized HSV color of daylight toward the sun, away from the sun, and sky under various conditions.

Sun angle	% of Cloud cover	Sun visibility	hsv_{sun}^{*}	hsv_{away}^{*}	hsv_{sky}^{*}
			0.5224	0.5466	0.5657
61-75	0-20	1	0.0503	0.2807	0.0606
			0.3398	0.3787	0.3430
			0.4848	0.3589	0.4329
61-75	21-50	1	0.0691	0.0884	0.0224
			0.3435	0.3470	0.3362
			0.4318	0.4026	0.5190
61-75	51-70	0.5	0.0440	0.0979	0.0638
			0.3400	0.3478	0.3437
			0.4998	0.3784	0.5264
61-75	71-100	0	0.0594	0.0599	0.0675
			0.3424	0.3441	0.3423

*hsv - normalized HSV color space.

A board having a number of matte surfaces of various colors is used for this purpose. The surface in the middle of the board is a calibrated matte white Munsell N/9 paper with maximum reflectivity of 98% and is used to sample the incident light. The board is mounted on an adjustable stand which could be varied from vertical to horizontal. The direction of the board could also be varied by changing the stand position. Any variation in the board orientation is done manually. A total of 390 images of the board (182 images toward the sun, 111 images away from the sun, and 97 images from the sky) have been taken under different conditions during several months. Also the camera is mounted on a tripod with angular markings of 15° along with a rotatable head mount with marking of 10°. A sample image of the board is shown in Figure 2. During data collection, the board standing position is changed to vary the viewing geometry; images were taken at every 10 to 15° change in the sun angle. The maximum possible variation of the light color for each day was captured under chosen conditions. And white surface color was sampled as the average color over 30 by 30 pixels area. The viewing geometry with respect to the white surface was approximately fixed by keeping a constant distance about 1 to 1.5 m between the camera and the surface, as well as a constant camera height being one and half meters. Table 1 shows a partial representation of the above color model.

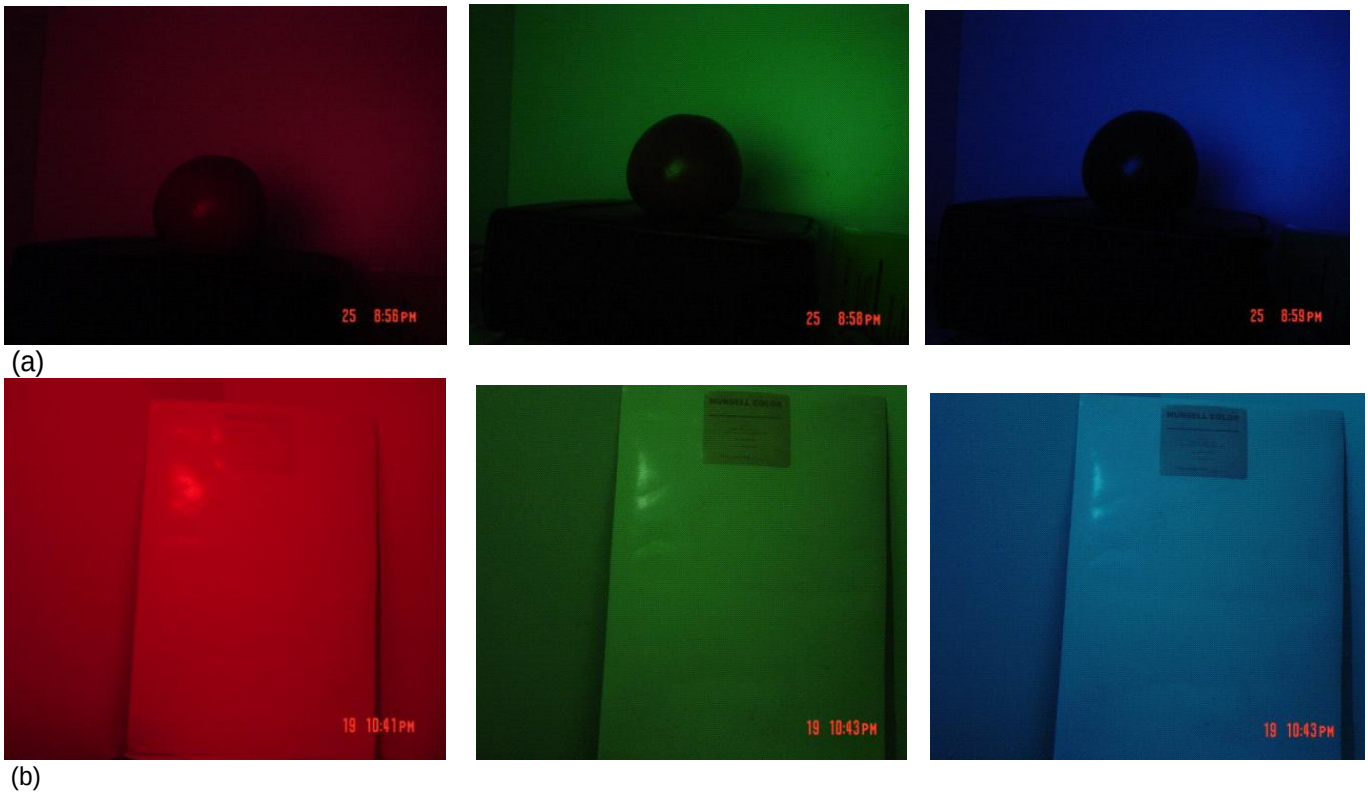

Figure 3. (a) Dark room images of red tomato Lambertian color estimation and (b) White Munsell paper under red, green, and blue lights.

Tomato Lambert color estimation

Based on Petrov's Lambertian color coefficient model (1993), the surface color can be written as the surface albedo color times the illuminant color. In mathematical forms it is shown as:

$$\begin{bmatrix} r \\ g \\ b \end{bmatrix} = \begin{bmatrix} W_{rr} & W_{rg} & W_{rb} \\ W_{gr} & W_{gg} & W_{gb} \\ W_{br} & W_{bg} & W_{bb} \end{bmatrix} \begin{bmatrix} r_i \\ g_i \\ b_i \end{bmatrix} \quad (2)$$

Where r_i, g_i, b_i are the color of the incident light and W_{rr} , W_{rg} , W_{rb} are the color coefficient or albedos of the red component of the surface under red, green, and blue bands of illuminant, respectively. The other expressions for g and b are analogous. So the apparent color of a Lambertian surface or the Lambertian component of a surface makes a linear transform of the incident light, the coefficient of which is determined by the spectral reflectance of the surface. The color of the illuminant is measured from the Munsell White paper under red, green, and blue lights and the color of the surface is also measured under three mentioned lights. As a result, a total of three images are needed for each surface, all taken in dark room. Measurements are put in equation (2) which will yield nine equations. Solving for the nine unknowns from the nine equations just obtained will result in color coefficient matrix for a specified surface. Using this albedo matrix and the color of the illuminant coming from the outdoor daylight table, the Lambertian color of the surface under that illuminant could be found again using equation (2). Figure 3 shows the dark room pictures for a sample tomato and the white Munsell paper under red, green, and blue lights. From the white Munsell surface, the color of the illuminating light is measured and from the tomato image under different lights, the lambertian color of the surface can also be found.

Reflectance Model: Normalized photometric function for tomato

Normalized Photometric Function (NPF) in HSV color space is a reflectance model for use in outdoor color images is developed based on the existing surface reflectance models. These reflectance models include Phong's reflectance model (1975), Nayar hybrid reflectance model Nayar et al. (1990), and Shafer's dichromatic model Shafer (1985). Since the assumptions made on these models are not suitable for outdoor images Buluswar and Draper (2002), a normalized photometric function in normalized HSV color space based on the previous reflectance models is built for use with the color model built above. NPF really plots the relative change in normalized color of a surface as the viewing angle changes. Three to five images are used to cover the full range of relative viewing angle of -90° to +90°. One image has to be at relative viewing angle of zero with the specular effect. The normalized HSV color of 17 pixels on the line passing through the centriod is found in normalized HSV to estimate NPF. Colors are mapped onto the xy coordinates. Also, the Lambertian and illuminant colors are mapped onto coordinates. Therefore, the normalized HSV distance of the measured color with respect to Lambert color of the surface could be found. The following three schematics shown in Figures 4 to 6 represent the NPFs for three different color tomatoes in this article.

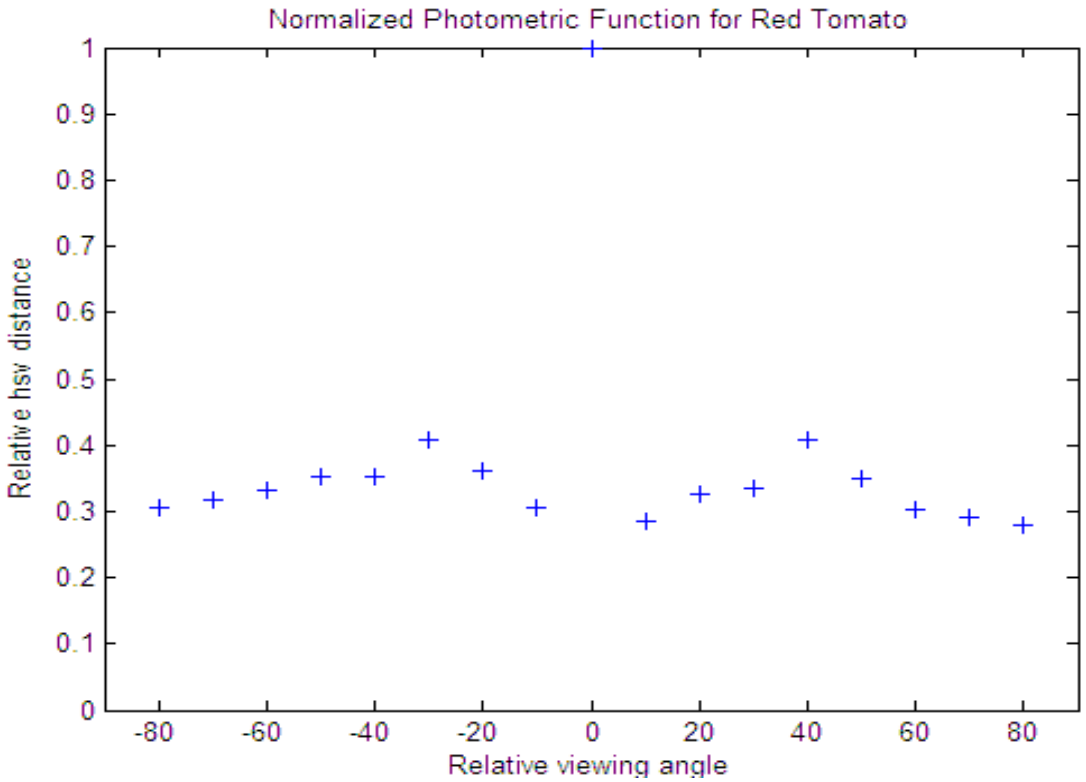

Figure 4. Normalized photometric functions for red tomato.

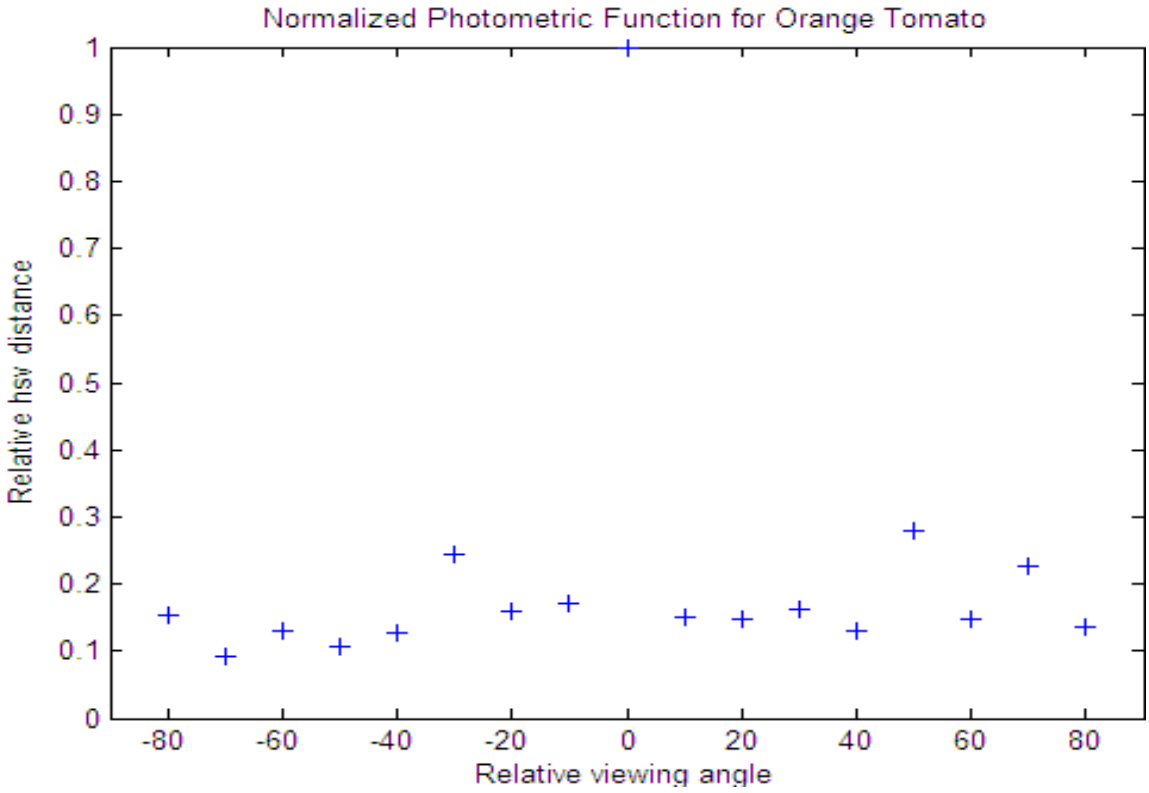

Figure 5. Normalized Photometric Functions for orange tomato.

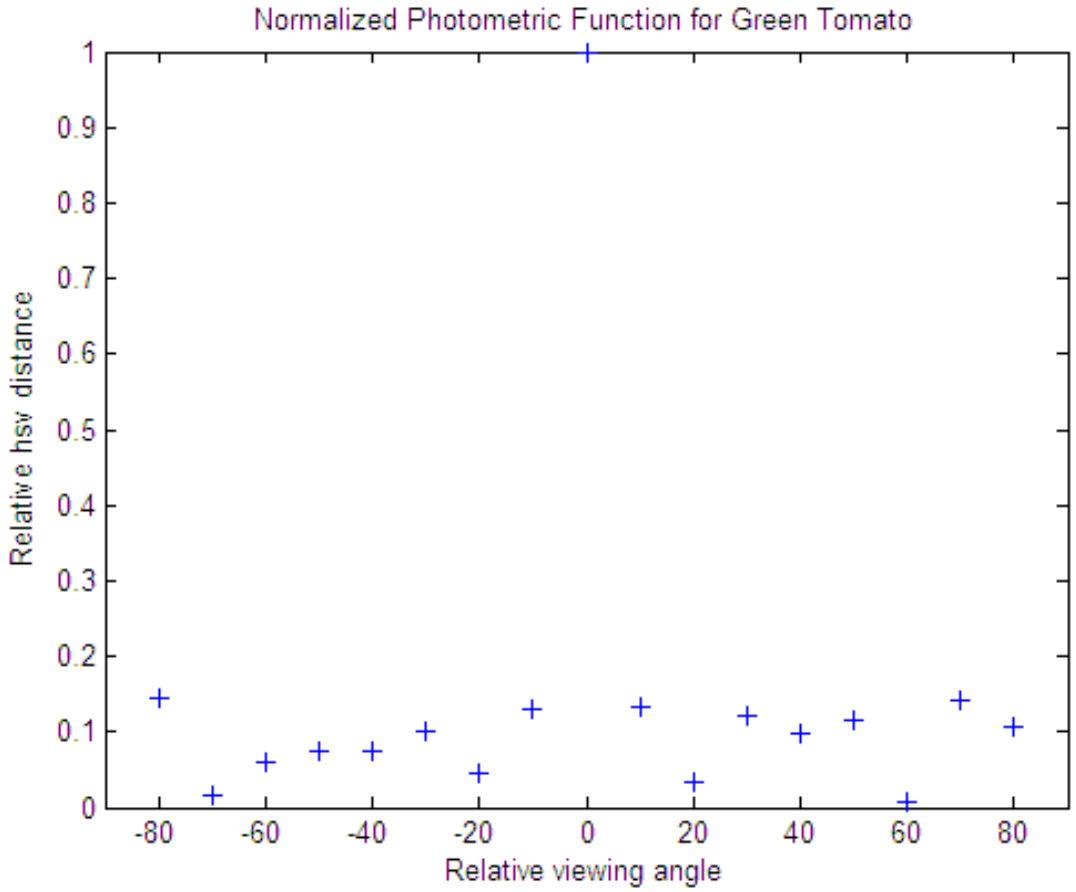

Figure 6. Normalized photometric functions for green tomato.

Estimating tomato color

Once the color of the illuminant (from the color model) and estimated Lambertian color of the tomato is known, the dichromatic line is established. The color of any pixels of tomato will be a color point and lie on this line connecting the diffuse and specular points. Normalized HSV color space is used and because of that, the color points are transferred into xy coordinates to be able to calculate the coordinates of any other color points and consequently do the reverse mapping and find the color in normalized HSV color space. The apparent color at any relative viewing angle is the base color which is Lambertian color plus the offset color a pixel has along the dichromatic line from the Lambert color.

EXPERIMENTAL RESULTS AND ANALYSIS

Here, the tomato surface spike effect detection and correction strategy using actual outdoor images for experiments and analysis and discussion on the experimental results is presented. The overall average computational time for tomato color correction is 2.48 s as compared to average performance time of 1.98 s for Chang and Tseng's algorithm (2011). Although, our method takes 0.5 s more time but the capability of our color based models are far more for other applications of outdoor.

Examples of applied steps

A database of 102 images is built. The images of red, orange, and green tomatoes were taken under different outdoor conditions on different days in Malaysia. It has been used to photograph tomato images under bright sun so it could create a good specular effect on its surface. A classifier is built to distinguish between the colors of the tomato as it will be needed in the treatment of color later on during the process. It is built based on the color of training images for each class of tomato color. The accuracy of this classifier is 94%. All the images of the database are color corrected and here a sample of the corrections is introduced. Then the aforementioned steps namely; the detection of spike region, thresholding and canny edge detection to find the tomato boundary to see if the spike pixels are on tomato surface, and then the color prediction of pixels to do the color correction are applied. Figures 7 to 9 show the results of these steps. No image processing or morphological operations have been applied to the resulted images since they are not for

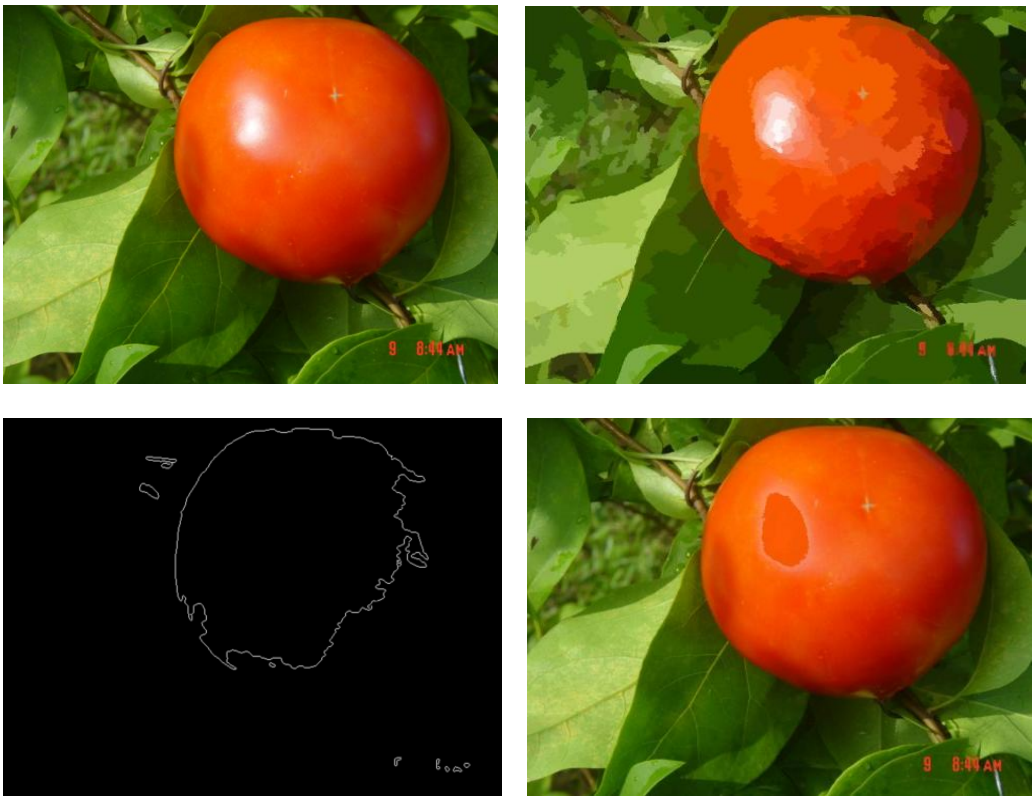

Figure 7. Outdoor red tomato image, segmented, edge detected, and color corrected images.

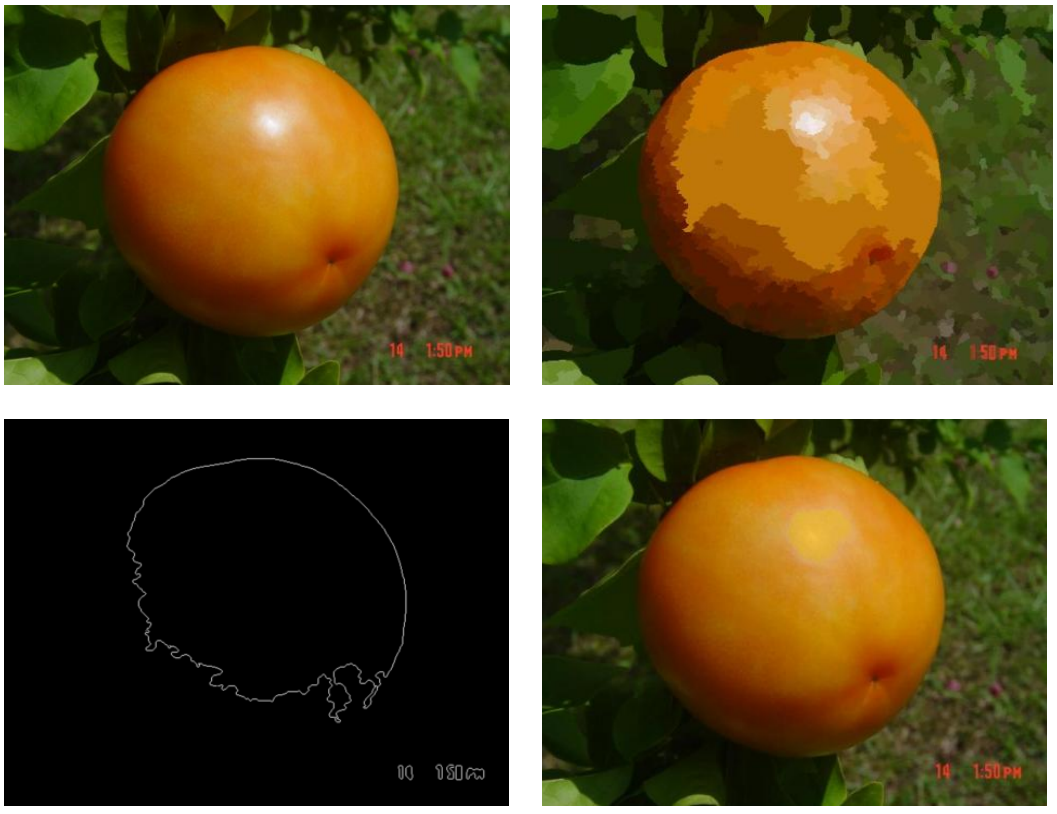

Figure 8. Outdoor orange tomato image, segmented, edge detected, and color corrected images.

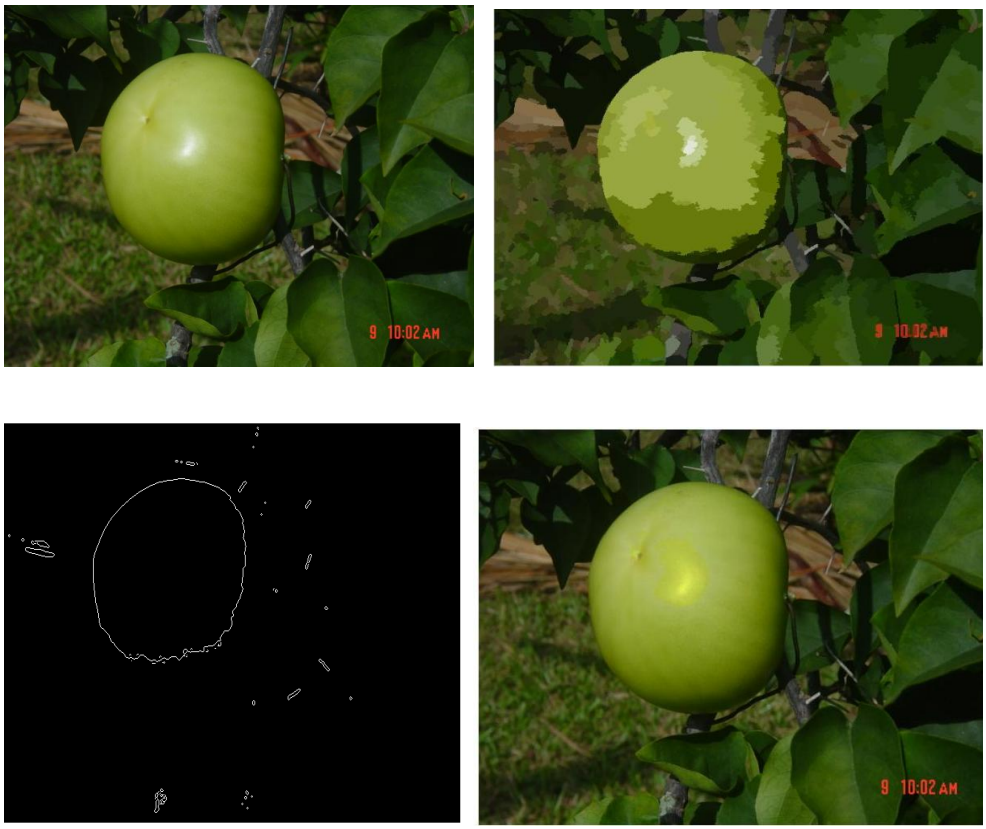

Figure 9. Outdoor green tomato image, segmented, edge detected, and color corrected images.

human visual purposes.

Comparison and analysis

A way to check the legitimacy of corrected color is to compare it against the tomato color itself. Under outdoor condition when the sun is shining, the tomato surface will be of many different colors. The causes could be the glossy skin of tomato, the tomato spherical shape, the tomato self shadowing effect, and its self reflection effect. Based on the models developed, the estimated color to be replaced for the spike region of tomato under sunlight (blue color in Figure 10) is best tested against the color of the rest of tomato region (red color in Figure 10) without the spike area. For this reason, histograms for images as shown in Figure 10 are created and checked to see if the estimated color falls within the confidence interval of the mean of the tomato color. Figures 10-12 show the color histograms of the sample images of Figures 7-9. For the 102 images taken, the accuracy for the red tomato color correction is 97%, orange tomato 86.5%, and green tomato is 95% which indicates the mean to be 93%. The reason for the low correction for the orange tomato is because the orange tomatoes used in the images throughout the experiments were not exactly the same color as the orange tomatoes being sampled in the beginning. Tomatoes change color over time especially orange tomatoes and it was the first orange tomato that is used to estimate the Lambert color.

Another reason could be the so called orange tomato having mixed colors of orange and green. This could change the color histogram and ultimately making the difference with the estimated color. It is proven that the predicted color is within the 2σ confidence interval and a valid color to be replaced for specular spike region on the surface of tomatoes.

CONCLUSION

Predicting outdoor color of objects is a challenging task and is very useful for outdoor machine vision. The color correction of tomato is as one application to the use of outdoor color model and surface reflection model developed here for tropical places. Another application could be in the field of smart farming for spraying plants. Obstacle recognition can also benefit from the models.

One of the major contributions of this study is to develop an automatic detection and correction procedure based on color-based models, detection, and correction algorithm. Experimental results provide evidence that the

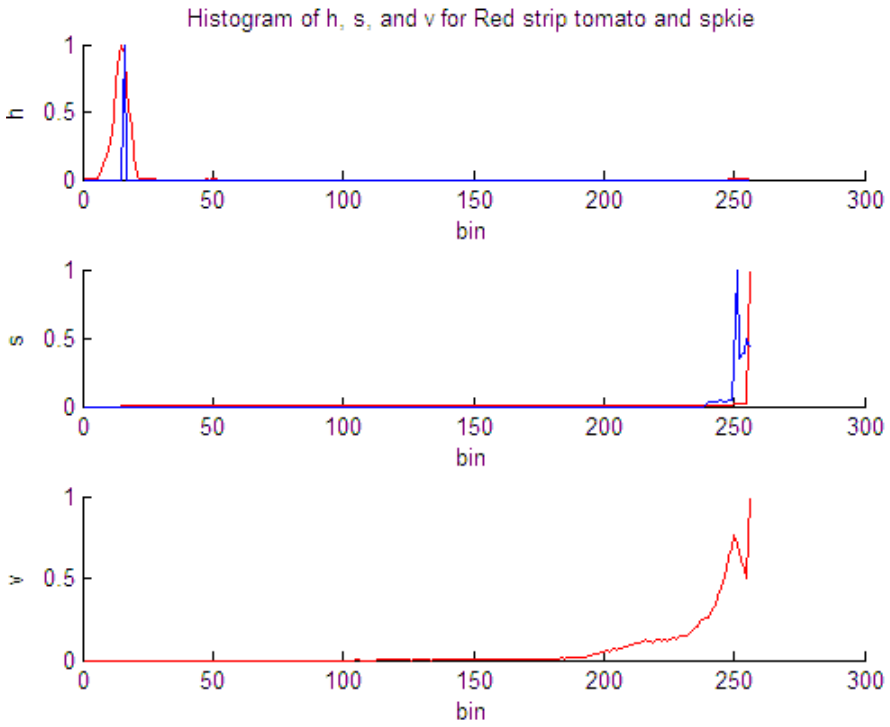

Figure 10. Color histograms for portion of tomato without the spike in red and the corrected color for the spike in blue for red.

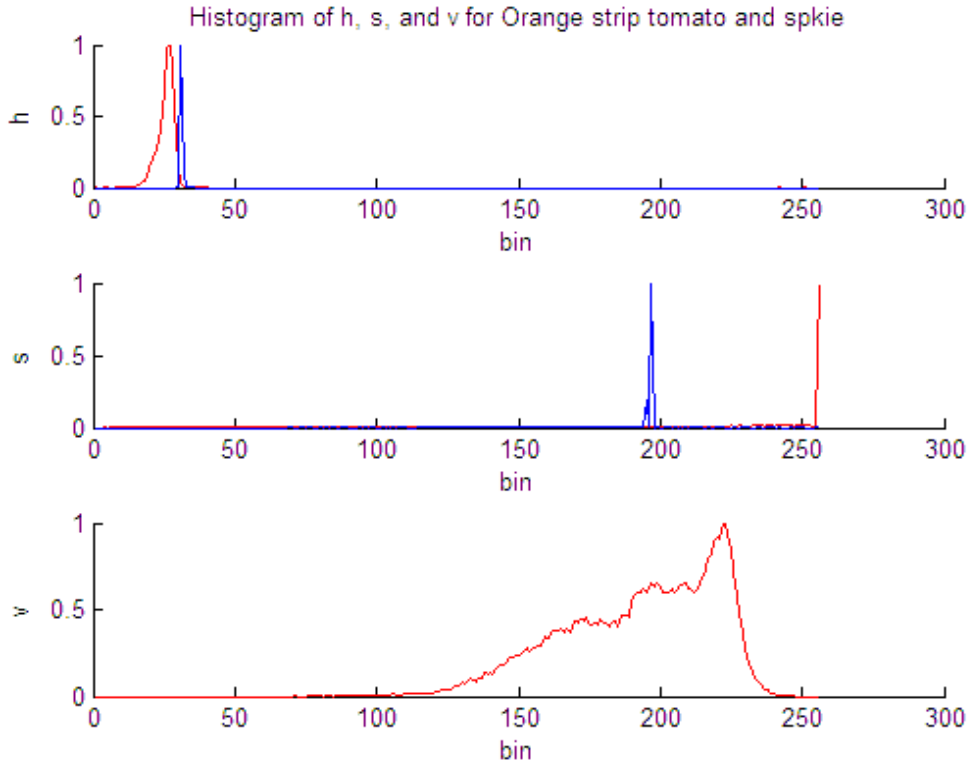

Figure 11. Color histograms for portion of tomato without the spike in red and the corrected color for the spike in blue for orange tomato.

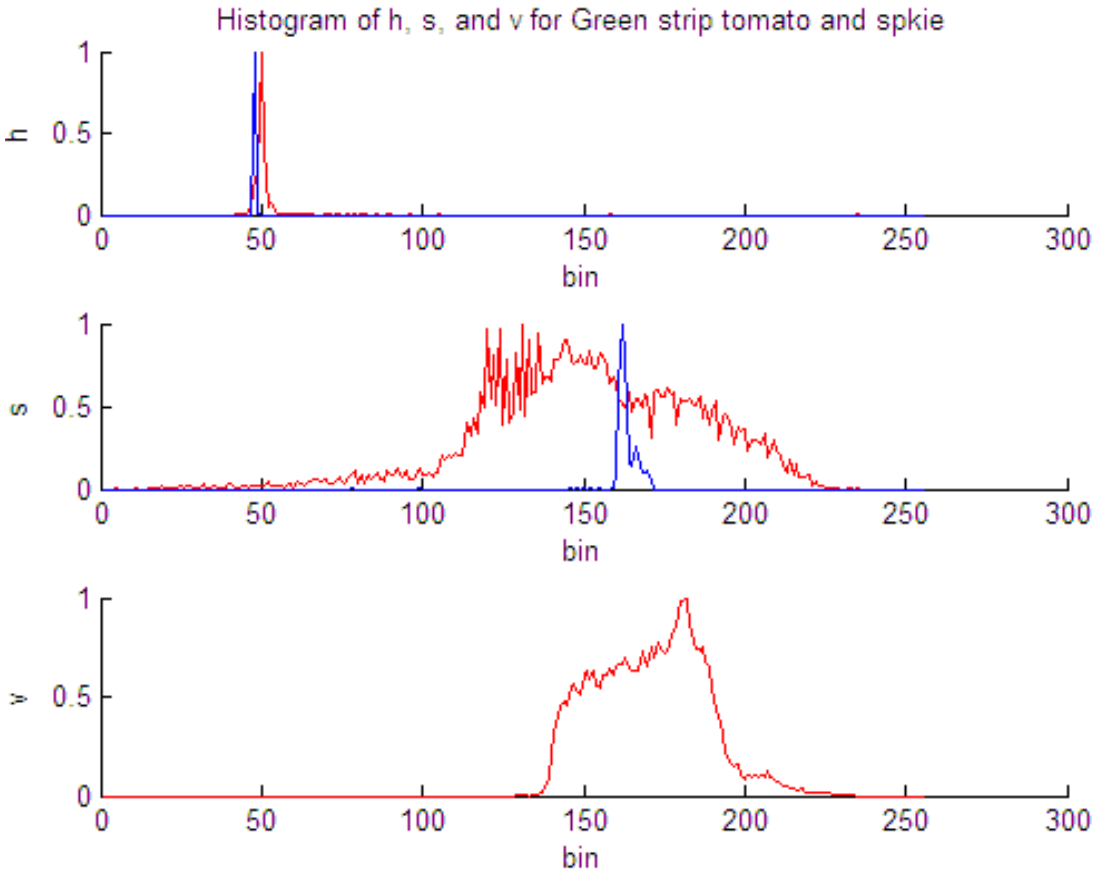

Figure 12. Color histograms for portion of tomato without the spike in red and the corrected color for the spike in blue green tomato.

proposed algorithm can produce valid results.

The overall high accuracy of tomato color recovery is due to correct functioning of both the tomato classifier and the daylight color model in Table 1. Of course the low errors contributed by the Lambertian color estimation, building NPF, and relative viewing angle have effects in achieving high accuracy for color recovery. The high accuracy of the tomato classifier plays an important role in the process of choosing the right path for the appropriate tomato color estimation. If that was not the case, there would be total failure.

As mentioned before the performance of our color correction algorithm is 0.5 s slower than the algorithm purposed by Chang and Tseng's detection and correction algorithm. Their method of correction is based on using the neighboring pixels to remove and correct the glossy effects caused due to the use of flash or low illumination. In their case the test images are taken under controlled illumination. But our images are taken in outdoor scenes under varying illumination and predict color of spiky pixels. The color correction algorithm in this study is only one of the applications of outdoor models developed. It can be used for autonomous driving, landmark detection, obstacle detection, and many others.

ACKNOWLEDGEMENTS

The authors would like to thank Mrs. Rosiah Osman for office support and Institute of Advanced Technology, University Putra Malaysia for providing the tools needed for practical experiments involved.

REFERENCES

Buluswar SD, Draper BA (2002). Color models for outdoor machine vision. J. Comput. Vis. Image Unders., 85(2): 71-99.

Chang RC, Tseng FC (2011). Automatic detection and correction for glossy reflections in digital photograph. J. Multimed., 6(2): 139-146.

Comaniciu D, Meer P (2002). Mean shift: A robust approach toward feature space analysis. IEEE Trans. Pattern Anal. Mach. Intell., 24(5): 603-619.

Lin S, Li Y, Kang SB,Tong X, Shuml HY (2002). Diffuse-Specular separation and depth recovery from image sequences. Proceed. Eur. Conf. Comput. Vis. Image Unders., pp. 210-224.

Nayar SK, Ikeuchi K, Kanade T (1990). Determining shape and reflectance of hybrid surfaces by photometric sampling. IEEE Trans. Robot. Autom., 6(4): 418-431.

Petrov AP (1993). Surface color and color constancy. Russian Scientific Center "Kurchatov Institute" Color Res. Appl., 18(4): 236-240.

Phong BT (1975). Illumination for computer generated pictures. Communications of the ACM, 18(6): 311-317.

Sahragard N, Abdul Rahman BR, Hamiruce MBM, Shattri BM (2011).

Color model for outdoor machine vision for tropical regions and its comparison with the CIE model. IOPConf. Series: Mater. Sci. Eng., 17: 012-046.
Shafer SA (1985). Using color to seperate reflection components. J. Color Res. Aappl., 10(4): 210-218.
Sojodishijani O,Rostami V,Abdul Rahman BR (2010). A video-rate color image segmentation using adaptive and statistical membership function. J. Sci. Res. Essays, 5(24): 3914-3925.
Tan RT,Ikeuchi K (2005a). Separating reflection components of textured surfaces using a single image. IEEE Trans. Pattern Anal. Mach. Intell., 27(2): 178-193.
Tan RT,Ikeuch K (2005b). Reflection components decomposition of textured surfaces using linear basis functions. Paper presented at the Proceedings of the IEEE Comput. Soc. Conf. Comput. Vis. Pattern Recognition, San Diego, CA., 1: 125-131
Tu Y,Yi F,Chen G, Jiang S,Huang Z (2010). Illumination removal in color images using retinex method based on advanced adaptive smoothing. IEEE, International Conference on E-Health Networking, Digital Ecosyst. Technol., 5496598: 219-223
Wu Y,Liu Z,Han Y,Zhang H (2010). An Image Illumination Correction Algorithm based on Tone Mapping. IEEE 3rd International Congress on Image and Signal Processing. CISP, 2(5647231): 645-648.